Fiber Alignment in Bioprinted Acoustically Responsive Scaffolds and COMSOL Drug Release Model

Ze Qi "Natalie" Chan

Faculty Advisors: Dr. Mitra Aliabouzar, PhD and Dr. Mario Fabiilli, PhD

Department of Biomedical Engineering, University of Michigan

ABSTRACT

Acoustically-responsive scaffolds (ARSs) are hydrogel scaffolds containing payload-carrying emulsions, the release of which can be non-invasively and spatiotemporally controlled using focused ultrasound, in a mechanism termed acoustic droplet vaporization (ADV). There is a need for a scaffold that can mimic the native extracellular matrix surrounding cells to facilitate cell migration and proliferation. This study aims to examine fiber alignment outcomes in bioprinted fibrinogen and hyaluronic acid-containing ARSs by varying printing parameters. Confocal images of the bioprinted scaffolds demonstrated that printing with high-gauge needles enabled the formation and alignment of fibers in these scaffolds.

Tissue regeneration can be stimulated by the cell and drug delivery from ARSs. Predictions of drug release over time by the ARS post-ADV are valuable in ensuring controlled dosing levels to surrounding tissue. We modelled the drug release profile from an ARS made of fibrin using COMSOL Multiphysics software. The model revealed a steady-state of 60% total drug release by the second day of release.

1. INTRODUCTION

Hydrogels are used in regenerative medicine for the delivery of cells and bioactive payloads like growth factors for tissue regeneration. They are capable of high water retention for cell delivery, and cell encapsulation within their porous network. However, a major challenge is fabricating a scaffold that can mimic the native extracellular matrix surrounding cells to facilitate biological processes like cell migration and proliferation.[1]

In recent years, 3D bioprinting has enabled the fabrication of hydrogel-based scaffolds with tunable mechanics and biomolecule release profiles.[2] The integration of computer-aided design (CAD) and additive manufacturing has enabled layer-by-layer deposition of biomaterial during extrusion-based bioprinting.[3] The properties of bioprinted scaffolds are dependent on the patterned geometries and mechanical properties of printed strands, which are essentially dependent on bioprinting parameters, including printing needle diameter, printhead extrusion pressure, printing speed and crosslinking conditions.

In this study, we developed a hydrogel-based scaffold consisting of fibrinogen and hyaluronic acid (HA) via bioprinting. We investigated the outcomes of fiber alignment in bioprinted fibrin-HA scaffolds as a function of printing parameters such as extrusion pressure, speed and needle gauge. Bioprinting-induced fiber alignment is likely a result of shear stress and shear thinning undergone by fibrinogen during extrusion.

Acoustically-responsive scaffolds (ARSs) are hydrogel scaffolds containing payload-carrying emulsions, the release of which can be non-invasively and spatiotemporally controlled using focused ultrasound, in a mechanism termed acoustic droplet vaporization (ADV).[4] Fluorescently labelled dextran molecules are typically used as payloads in in vitro studies. Modelling kinetic release of drug from the ARS post-ADV would be significant to predicting drug dosing levels. We constructed a diffusion model to examine the drug diffusion profile. The model describes drug release from a fibrin hydrogel scaffold into a media surrounding the scaffold. The ultimate aim of this study is to model drug release from a drug-loaded fibrin hydrogel implant to surrounding tissue post-ADV to predict the drug loading and time needed to achieve adequate drug levels in the surrounding tissue.

---

[1] A. Salerno, P.A. Netti. "Review on computer-aided design and manufacturing of drug delivery scaffolds for cell guidance and tissue regeneration." Front. Bioeng. Biotechnol., 9 (2021), p. 519.

[2] D.B. Kolesky, K.A. Homan, M.A. Skylar-Scott, J.A. Lewis. "Three-dimensional bioprinting of thick vascularized tissues." Proc. Natl. Acad. Sci. Unit. States Am., 113 (12) (2016), pp. 3179-3184.

[3] J.K. Placone, A.J. Engler. "Recent advances in extrusion-based 3D printing for biomedical applications." Adv. Healthc. Mater., 7 (8) (2018), Article 1701161.

[4] O.D. Kripfgans, J.B. Fowlkes, D.L. Miller, O.P. Eldevik, P.L. Carson. "Acoustic droplet vaporization for therapeutic and diagnostic applications." Ultrasound Med. Biol., 26 (7) (2000), pp. 1177-1189.

2. METHODS

2.1 Bioink preparation

HA sodium salt from *Streptococcus equi* was dissolved in PBS at 14mg/mL by stirring at 350 rpm overnight. Fibrinogen solution was prepared by reconstituting bovine fibrinogen in PBS at 40mg/mL clottable protein. These solutions were also supplemented with 0.2U/mL aprotonin that has an activity of 7U/mL, then vortex mixed for 30 seconds. The solution was then degassed in a vacuum chamber at room temperature at 6kPa for 60 minutes to remove dissolved gas. Equal volumes of HA and fibrinogen solutions were combined with (30µL/mL) Alexa Fluor 647 dye by gentle stirring at 70rpm for 45 minutes. Bioinks were then transferred into 3mL and kept at 4°C until use. A conventionally-made gel structure is made by filling a well in a 24-well plate with 1.5mL of fibrinogen solution and thrombin solution, then left to polymerize for 30 minutes.

2.2 Cross-linking solution preparation

Bovine thrombin solution diluted with DPBS at 50U/mL.

2.3 3D bioprinting setup and process

The printed 10mmx10mmx1mm cuboid structure used in this report is from a CAD model readily programmed into the 3D bioprinter. These structures have a grid pattern of 90% infill density. All samples were printed using 3mL pneumatic printheads at room temperature through 30-gauge (internal diameters 150µm) steel-tipped needles. Printing parameter (extrusion pressure and printing speed) configurations were varied to assess fibrin fiber alignment. All samples were printed onto plastic 6-well plates.

Cross-linking solution was sprayed after deposition of each printed layer to ensure structural integrity of the samples during bioprinting. After printing, samples were submerged in a crosslinking solution to polymerize for 30 minutes.

2.4 Optical imaging and analyses

Conventionally-made and bioprinted samples were imaged using a confocal microscope with 40x water-immersion objective lens. Fiber orientation inside the samples were measured using the orientation distribution function of ImageJ.

2.5 COMSOL Multiphysics Model

‘Transport of Diluted Species’ physics was used to simulate a biomaterial matrix domain encased in an overlying media domain.

2.5.1 Model Geometry and Mesh Generation

Fig.1A illustrates the 2D geometrical construct representing a biomaterial matrix topped with overlying media (water). Dimensions of the model are based on conventionally-made fibrin gels deposited in a 24-well plate. The mesh element size was set to ‘Fine’ with a maximum element size limit of 0.1. Boundary layers were also defined at the borders interfacing the biomaterial and the surrounding media (Fig.1B). The simulation was executed over 10 days; data was collected at 1-day increments.

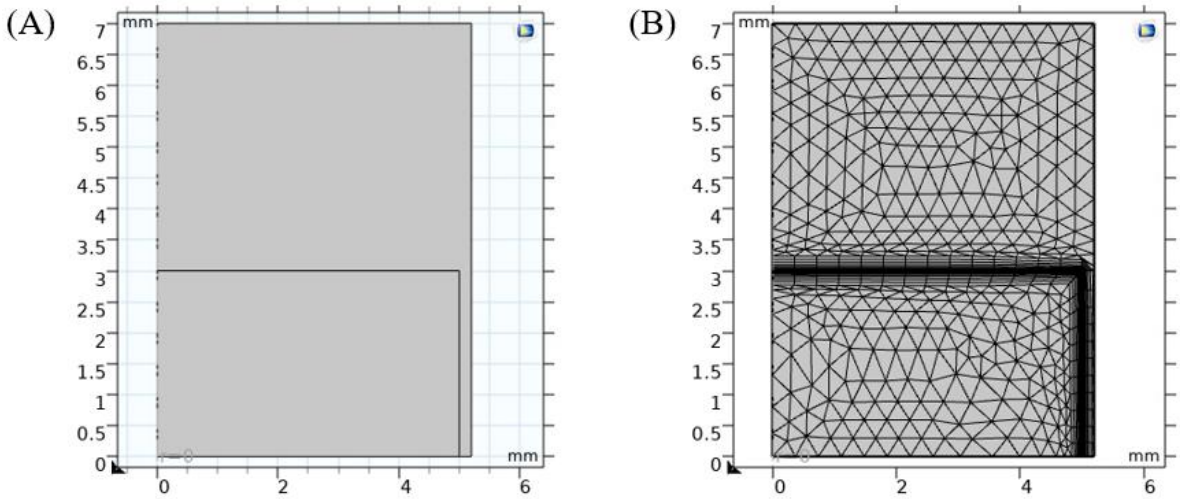

Fig.1. (A) Geometry and (B) mesh generation of the model in COMSOL Multiphysics.

2.5.2 Species transport equation:

$$\frac{\partial c_i}{\partial t} + \nabla \cdot (-D_{ik} \nabla c_i) = R_{ik}$$

This equation resolves the time-dependent mass balance for the concentration c_i of Dextran molecules. D_{ik} represents the diffusion coefficient of Dextran molecules in the respective medium *k*, where *k* is either the biomaterial matrix or overlying media. R_{ik} is the rate expression for Dextran molecule in medium *k*. The drug species in this study is not considered to participate in any chemical reaction, so R_{ik} is zero.

2.5.3 Boundary conditions and initial conditions

Axial symmetry was applied along the rotational axis. A no-flux boundary condition was applied to exterior boundaries on the geometry.

3. RESULTS AND DISCUSSION

3.1 Fiber alignment distribution

Confocal images of conventionally prepared fibrin-HA scaffold (Fig.2A1) exhibited random orientation of large fibrin domains, described by a broad distribution of orientation from -50° to 50° (Fig.2A2). Meanwhile, bioprinted fibrin-HA scaffolds resulted in fibrin fiber alignment, categorized simply as sparse (Fig.2B1) and abundant (Fig.2C1) populations of aligned fibers which have significantly narrower distributions of orientation, -50° to 10° and -60° to 0°, respectively. This demonstrates that bioprinting with high-gauge needles can produce regions of aligned fibers, presumed to be in the direction of printing. One hypothesis to explain the inconsistent populations of aligned fibers is that printed fibers revert to random orientations before cross-linking solution is sprayed onto the deposited layers. A possible method to overcome this is to print in a support bath containing the cross-linking solution, so that the fibers are immobilized upon extrusion.

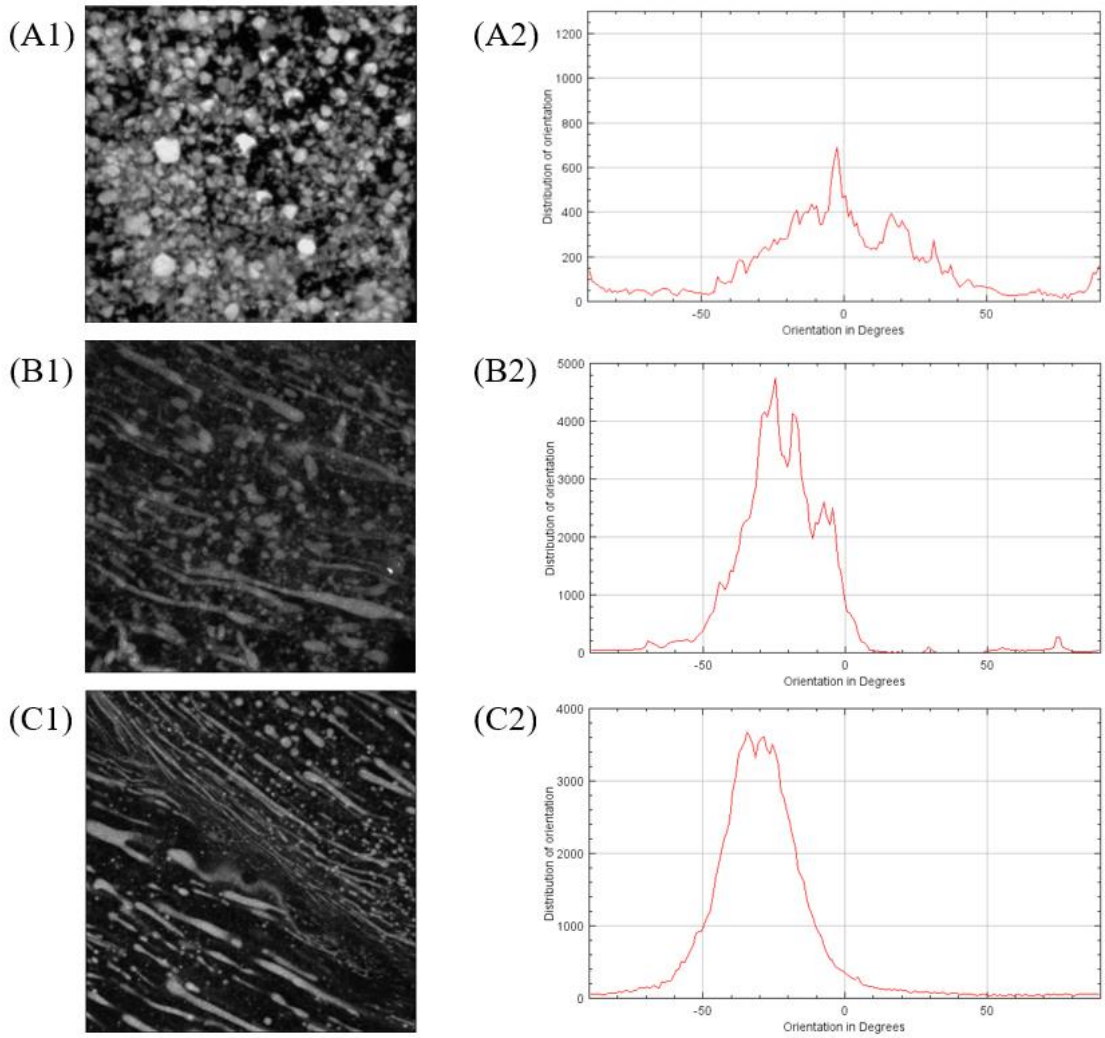

Fig.2. Bioprinting enabled the formation of aligned fibers. (A) Conventionally prepared fibrin-HA scaffolds displayed random fiber orientation. Bioprinted scaffolds displayed (B) sparse and (C) abundant populations of aligned fibers.

3.2 Drug release model

Results of the COMSOL model simulation were displayed as color-coded release profiles (Fig.3), and a percentage release profile over a period of 10 days (Fig.4). The results show that a steady state of 60% release is reached at approximately 2 days of release.

To validate the model, the results for percentage release profiles were compared to experimental data from complementary in vitro experiments (Fig.4). The modelled release rate was significantly greater than that of the experimental value, and the overall release was greater in the simulated model compared to the experimental release at 47%. This large discrepancy could be attributed to the stochastic nature of gas bubble formation upon application of ultrasound to the ARS; not all emulsions vaporize during the experiment, thus not all drug is available for release from the scaffold.

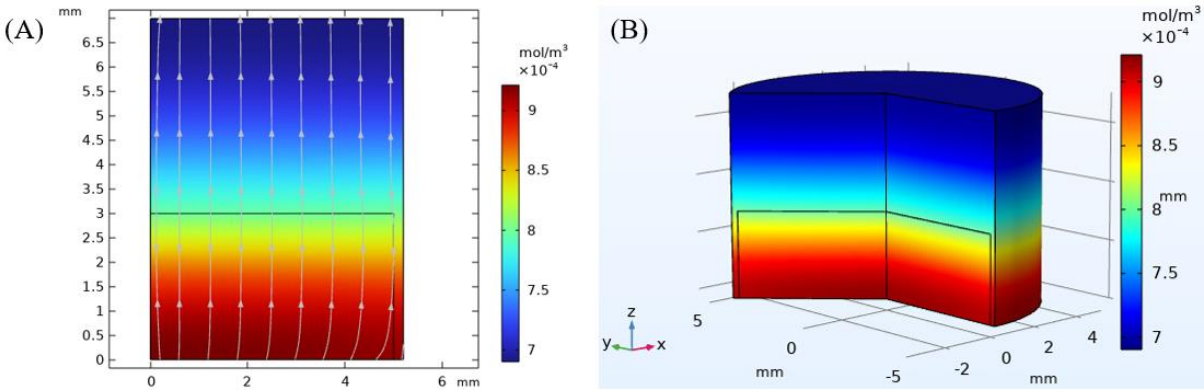

Fig.3. (A) 2D and (B) 3D surface plots of drug diffusion simulation at 1 day of release. Streamlines demonstrate upward diffusion of drug molecules from the biomaterial matrix domain into the overlying media domain.

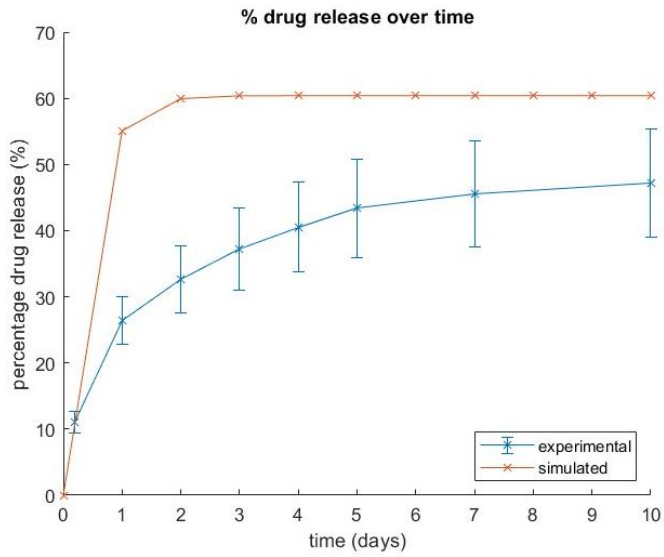

Fig.4. Drug release profiles of both simulated models and experimental results.

4. FUTURE WORK

There are plans within the lab to bioprint fibrinogen-HA loaded with breast cancer cells to study microenvironmental effects on breast cancer cell migration within the scaffold. Before moving forward with making cell-laden bioinks, the next step would be to investigate fiber alignment distributions in fibrin-HA scaffolds bioprinted using low-gauge needles. It would be valuable to determine the degree to which needle gauge, printing speed and printing pressure influence fiber alignment within bioprinted scaffolds. Furthermore, the protocol for fabricating these scaffolds require optimization to ensure consistent fiber formation throughout the construct.

In order to better represent the mechanisms of drug release from a fibrin hydrogel scaffold, the next step in advancing the simulated model would be to incorporate porosity in the biomaterial matrix domain. This can be done using the 'Transport of Diluted Species in Porous Media' physics node. A parametric study shall also be conducted to investigate the trend between rate of drug release and porosity of the biomaterial. Once this model is refined, the application of ultrasound to the scaffold will also be modelled to simulate ADV, which triggers the start of drug release kinetics.

ACKNOWLEDGMENTS

Thank you to Dr. Mario Fabiilli and Dr. Mitra Aliabouzar for providing me the opportunity to conduct research in the Fabiilli Laboratory and Aliabouzar Laboratory. A special thank you to Dr. Mitra Aliabouzar for the support and valuable guidance throughout the project.

I wish to extend my sincere gratitude to Mr. Tony Wang for his generous support. This award has granted me the opportunity to continue making progress on research projects and pursue my academic interests in the field.

REFERENCES

1. Salerno, P.A. Netti. “Review on computer-aided design and manufacturing of drug delivery scaffolds for cell guidance and tissue regeneration.” Front. Bioeng. Biotechnol., 9 (2021), p. 519.

2. D.B. Kolesky, K.A. Homan, M.A. Skylar-Scott, J.A. Lewis. “Three-dimensional bioprinting of thick vascularized tissues.” Proc. Natl. Acad. Sci. Unit. States Am., 113 (12) (2016), pp. 3179-3184.

3. J.K. Placone, A.J. Engler. “Recent advances in extrusion-based 3D printing for biomedical applications.” Adv. Healthc. Mater., 7 (8) (2018), Article 1701161.

4. O.D. Kripfgans, J.B. Fowlkes, D.L. Miller, O.P. Eldevik, P.L. Carson. “Acoustic droplet vaporization for therapeutic and diagnostic applications.” Ultrasound Med. Biol., 26 (7) (2000), pp. 1177-1189.